Identification of host cell factors required for intoxication through use of modified cholera toxin

Carla P. Guimaraes,[1] Jan E. Carette,[1] Malini Varadarajan,[1] John Antos,[1] Maximilian W. Popp,[1] Eric Spooner,[1] Thijn R. Brummelkamp,[1] and Hidde L. Ploegh[1,2]

[1]Whitehead Institute for Biomedical Research, Cambridge, MA 02142
[2]Department of Biology, Massachusetts Institute of Technology, Cambridge, MA 02139

We describe a novel labeling strategy to site-specifically attach fluorophores, biotin, and proteins to the C terminus of the A1 subunit (CTA1) of cholera toxin (CTx) in an otherwise correctly assembled and active CTx complex. Using a biotinylated N-linked glycosylation reporter peptide attached to CTA1, we provide direct evidence that ~12% of the internalized CTA1 pool reaches the ER. We also explored the sortase labeling method to attach the catalytic subunit of diphtheria toxin as a toxic warhead to CTA1, thus converting CTx into a cytolethal toxin. This new toxin conjugate enabled us to conduct a genetic screen in human cells, which identified *ST3GAL5*, *SLC35A2*, *B3GALT4*, *UGCG*, and *ELF4* as genes essential for CTx intoxication. The first four encode proteins involved in the synthesis of gangliosides, which are known receptors for CTx. Identification and isolation of the *ST3GAL5* and *SLC35A2* mutant clonal cells uncover a previously unappreciated differential contribution of gangliosides to intoxication by CTx.

Introduction

Cholera holotoxin (CTx) is an AB_5-type toxin, with its five B subunits assembled in a ring-shaped structure and the C terminus of the A subunit protruding through the central pore (Fig. 1; Zhang et al., 1995). Each of the B subunits can bind to the surface monosialoganglioside GM1 and so allow internalization of CTx into host cells (Heyningen, 1974; Fujinaga et al., 2003). The A subunit projects above the plane of the B pentamer and exposes a protease-sensitive loop, stabilized by a single intramolecular disulfide bond (Zhang et al., 1995). Cleavage of this loop by bacterial and cell host proteases yields two distinct chains (CTA1 and CTA2) that remain connected via the disulfide bond, reduction of which is required for toxicity (Mekalanos et al., 1979). The CTA1 chain ADP-ribosylates the α subunit of the heterotrimeric GTP-binding protein Gs, triggering a series of events that lead to the opening of the chloride channels at the plasma membrane, with concomitant secretion of chloride and water (Schafer et al., 1970; Kassis et al., 1982; Kahn and Gilman, 1984). In the intoxicated cell, only CTA1 reaches the cytoplasm to interact with its substrates (Fujinaga et al., 2003), but how CTA1 separates from the holotoxin is unclear, as is the identity of the channel via which CTA1 translocates across membranes. The prevailing view is that upon binding of the B-pentamer to GM1 at the cell surface, CTx is endocytosed and reaches the ER (for review see Lencer and Tsai, 2003; Wernick et al., 2010b). The intramolecular disulfide bond is then reduced, a reaction that can be catalyzed by PDI, at least in in vitro reactions (Majoul et al., 1997; Orlandi, 1997; Tsai et al., 2001). CTA1 dissociates from the remainder of the complex to allow translocation into the cytoplasm. CTA1 may co-opt mechanisms used in the ER to translocate misfolded proteins from the lumen of the organelle to the cytoplasm (Hazes and Read, 1997), a process referred to as dislocation. However, direct biochemical evidence for trafficking of CTA1 through the ER is lacking, and the identity of the portals via which CTA1 is translocated remain elusive.

The importance of dissecting the intoxication pathway of CTA1 goes beyond its impact on understanding the etiology of cholera disease. Because no host factor presumably evolved to afford pathogens a selective advantage, toxins must exploit host

Correspondence to Hidde L. Ploegh: ploegh@wi.mit.edu

J.E. Carette's present address is Dept. of Microbiology and Immunology, Stanford University School of Medicine, Stanford, CA 94305.

T.R. Brummelkamp's present address is the Netherlands Cancer Institute, 1066 CX Amsterdam, The Netherlands.

Abbreviations used in this paper: CTx, cholera holotoxin; CTB, B subunit of CTx; DTA, catalytic subunit of DTx; DTx, diphtheria toxin; E/L, endosomal/lysomal; LB, lysogeny broth; MS/MS, tandem mass spectrometry; PI, propidium iodide.

The Rockefeller University Press $30.00
J. Cell Biol. Vol. 195 No. 5 751–764
www.jcb.org/cgi/doi/10.1083/jcb.201108103

Figure 1. **Schematic representation of the structure of CTx and of the strategy used to attach, in a site-specific manner, peptides or proteins to CTA1 in the context of the pre-assembled holotoxin.**

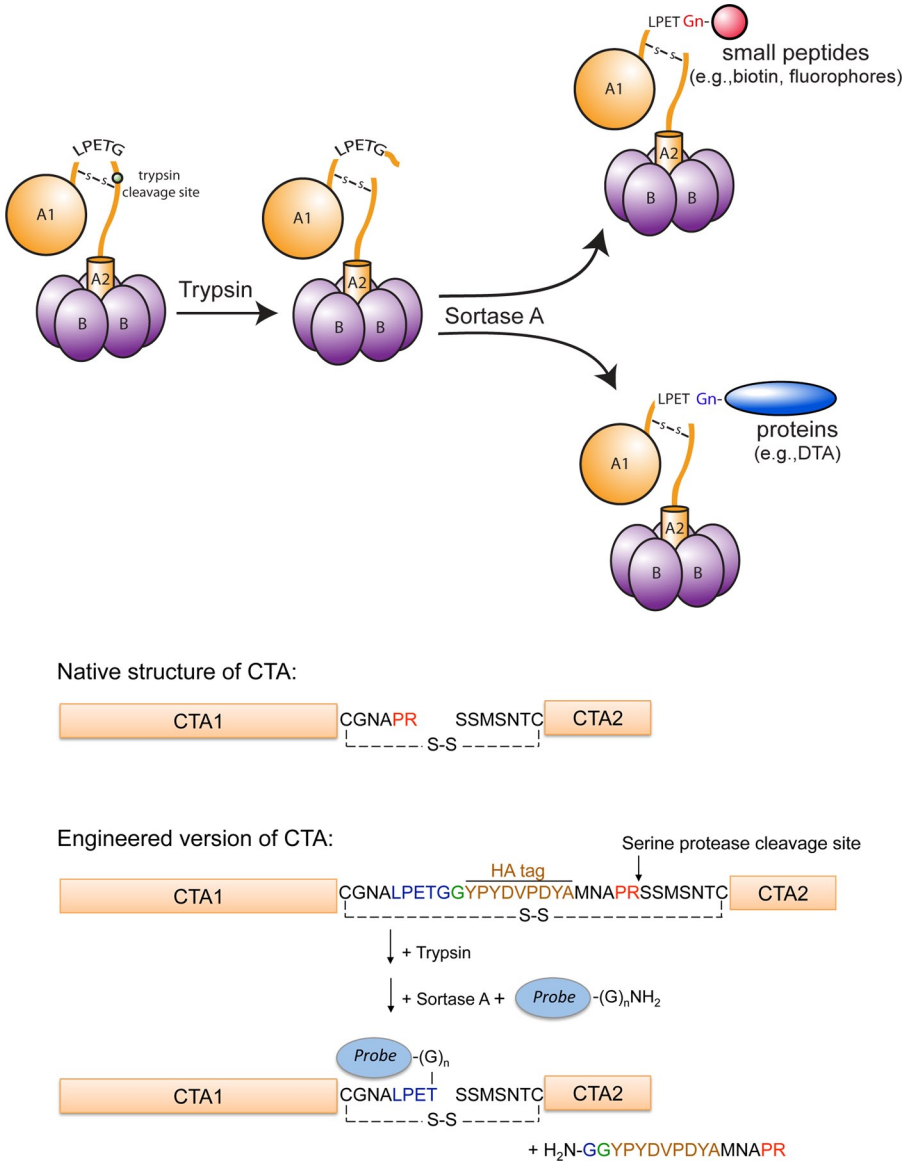

molecular machinery to intoxicate cells. Unraveling how toxins traffic from one intracellular compartment to another and across subcellular membranes provides valuable information about how the mammalian cell operates. However, the difficulties inherent in labeling CTx or CTx structural-related toxins without loss of activity limit their use as research tools. Extension of the N terminus of CTA1 leads to its rapid degradation (Wernick et al., 2010a), and attempts to install, by genetic means, sizable protein fragments or intact proteins such as GFP in the A subunit loop have failed, presumably because such operations preclude assembly of active holotoxin. The strategies currently available to examine trafficking of CTA1 are limited to the use of polyclonal antibodies (Wernick et al., 2010a), circular dichroism/fluorescence, or Fourier transform infrared spectroscopy studies (Pande et al., 2007; Taylor et al., 2011), and to indicators of toxic activity such as loss of transepithelial resistance in polarized cell monolayers (Lencer et al., 1992), increased levels of cAMP (Kassis et al., 1982), or induction of morphological alterations in cells in culture (Guerrant et al., 1974; Donta et al., 1976) and in zebrafish embryos (Saslowsky et al., 2010). Although methods to chemically label CTx with fluorophores for cell imaging have been described, they do not yield homogenous populations of labeled CTx (Bastiaens et al., 1996; Bacia et al., 2002), making it difficult to equate distribution of fluorescence with that of active CTA1. The use of inhibitors of intracellular trafficking, such as brefeldin A (Lencer et al., 1993; Nambiar et al., 1993; Orlandi et al., 1993), are consistent with experiments using isolated microsomes (Schmitz et al., 2000) and transfected mammalian cells that overexpress CTA1 targeted to the ER by means of a cleavable signal sequence (Teter et al., 2002). All of these experiments implicate a role for the ER in intoxication. However it is not clear whether these models accurately capture the physiological sequence of events because the cotranslational mode of ER entry differs from that of normal delivery routes for CTA1 and further assumes that the ER is the relevant exit portal. Thus, strategies to site-specifically and quantitatively label the toxic CTA1 chain in the context of a functional holotoxin would help to directly address its intracellular trafficking.

Labeling through chemical modification, although convenient and straightforward, is rarely quantitative or site-specific. Modification of multiple surface-exposed amino acid side chains might compromise trafficking behavior or biological activity of CTx. A further complication is the paucity of exposed lysine or cysteine residues that lend themselves to chemical modification on CTA1. Also, the quaternary structure of the holotoxin is maintained only under mild conditions of labeling, not necessarily compatible with efficient chemical modification of CTx. Recently developed enzymatic methods for protein modification require either installation of sizable catalytic tags (such as SNAP-tags, 20 kD; Keppler et al., 2003) that cannot be genetically engineered into the CTA subunit loop without compromising holotoxin assembly, or installation of the 15–amino acid BirA acceptor peptide (Chen et al., 2005), the use of which is limited to the enzymatic installation of biotin and its synthetically challenging derivatives. To overcome these hurdles and to achieve efficient site-specific labeling of CTx, we have exploited the bacterial enzyme sortase A from *Staphylococcus aureus*.

Sortase A recognizes and cleaves a specific short motif, LPXTG (where X is any amino acid), appended to the protein of interest (Navarre and Schneewind, 1994). Cleavage occurs between the threonine and glycine residues, with the concomitant formation of an acyl enzyme intermediate between the enzyme and its substrate. This intermediate can be resolved via nucleophilic attack by an added oligoglycine peptide, resulting in the formation of a covalent bond with the LPXTG-containing protein at the site of cleavage. Because the oligoglycine peptide tolerates decoration with any substituent of choice, the final product can be labeled with a fluorophore, a photoaffinity probe, lipids, photocrosslinkers, or even other polypeptides (Ton-That et al., 1999; Popp et al., 2007; Antos et al., 2008; Tsukiji and Nagamune, 2009; Popp and Ploegh, 2011).

We cloned the sortase A recognition motif into the A subunit loop of CTx and devised a strategy to enable site-specific attachment of molecules to the C terminus of the catalytic CTA1 subunit in an otherwise preassembled and correctly folded CTx. Here, we exploit this method not only to create a version of CTA1 that reports on its possible delivery to the ER, but also to convert CTx from a toxin that merely elevates cAMP levels into a cytolethal entity for use as the selecting agent in a genetic screen in human haploid cells (Carette et al., 2009, 2011). This approach identified host factors essential for intoxication by CTx and allowed isolation of mutant cells with defects along the biosynthetic pathway of gangliosides. Our results shed new light on the role of various ganglioside synthetic pathways in the construction of receptors for CTx.

Results

Strategy to specifically label the C terminus of CTA1 in the context of the holotoxin

A sortase-catalyzed reaction requires exposure of the recognition sequence in a flexible/unstructured region (Popp et al., 2007). Based on the available crystal structure of CTx (Zhang et al., 1995), the loop formed by the intramolecular disulfide bond (Cys187-199) in the A subunit meets this criterion. Because cleavage between Arg192 and Ser193 is a prerequisite for full toxicity (Mekalanos et al., 1979), we installed a sortase A recognition motif (LPETG) immediately preceding Pro191. The LPETG sequence was followed by a glycine residue, an HA epitope tag, and a trypsin cleavage site (Fig. 1). Upon completion of the sortase reaction, the sequence of the final product is quite similar to that of the cleaved native version of CTx, carrying two additional amino acids at the predicted C terminus of CTA1, with the four C-terminal residues of CTA1 differing from native CTA1 (Fig. 1).

The LPETG-containing A subunit sequence and the native B subunit of cholera toxin were coexpressed using a bicistronic bacterial vector. Both proteins were equipped with signal sequences from the *Escherichia coli* heat-labile enterotoxin, synthesized as precursors, and delivered to the periplasm, where they are processed and assembled (Jobling et al., 1997). We purified the holotoxin by exploiting the intrinsic ability of the B-subunit to bind to Ni^{2+} (Dertzbaugh and Cox, 1998), followed by anion-exchange chromatography to resolve the AB_5 complex from the B pentamer (Fig. 2, A and B).

To determine whether extension of the loop was still compatible with formation of the intramolecular disulfide bond, we analyzed our modified version of CTx by SDS-PAGE under reducing and nonreducing conditions (Fig. 2 C). Upon incubation with trypsin, the 29-kD CTA (CTA1 + CTA2) polypeptide shifts to 24 kD only under reducing conditions (Fig. 2 C, +trypsin, compare with ±DTT); this 24-kD species corresponds to CTA1 separated from CTA2. We attribute the slight difference in mobility observed for CTA under nonreducing conditions (Fig. 2 C, compare ±trypsin and −DTT) to a change in SDS binding and shape, caused by the opening of the loop by trypsin. Altogether, this shows that the LPETG-containing version of CTx retains the ability to fold into the native structure. This toxin preparation also retains biological activity, as we found it indistinguishable from the unmodified CTx at eliciting morphological aberrations in Vero cells, even at low concentrations (Fig. 2 D).

Installation of small peptides at the C terminus of CTA1

Our initial attempts to label the modified CTx version showed that sortase A was inefficient at cleaving the LPETG-containing loop. Although flexible, the loop region might still impose constraints that hinder proper exposure of the sortase recognition motif. We solved this issue by using trypsin (EC 3.4.21.4) to nick the loop before the sortase reaction (Fig. 1). Sortase-mediated reaction conditions to label CTA1 were optimized using short oligoglycine peptides that contained either a biotin or a fluorophore (Fig. 3, A and B, top panels; and Fig. S1). We monitored labeling by SDS-PAGE/fluorescence imaging (for Alexa Fluor 647) or SDS-PAGE/immunoblotting (for biotin; Fig. 3, A and B, bottom). Because the HA tag is located C-terminally to the LPETG site, it is removed upon cleavage by sortase (Fig. 1, bottom). The extent of labeling can thus be assessed by the loss of anti-HA immunoreactivity. However, loss of the HA tag could also result from hydrolysis of the acyl-enzyme intermediate without formation of a labeled CTA1 product.

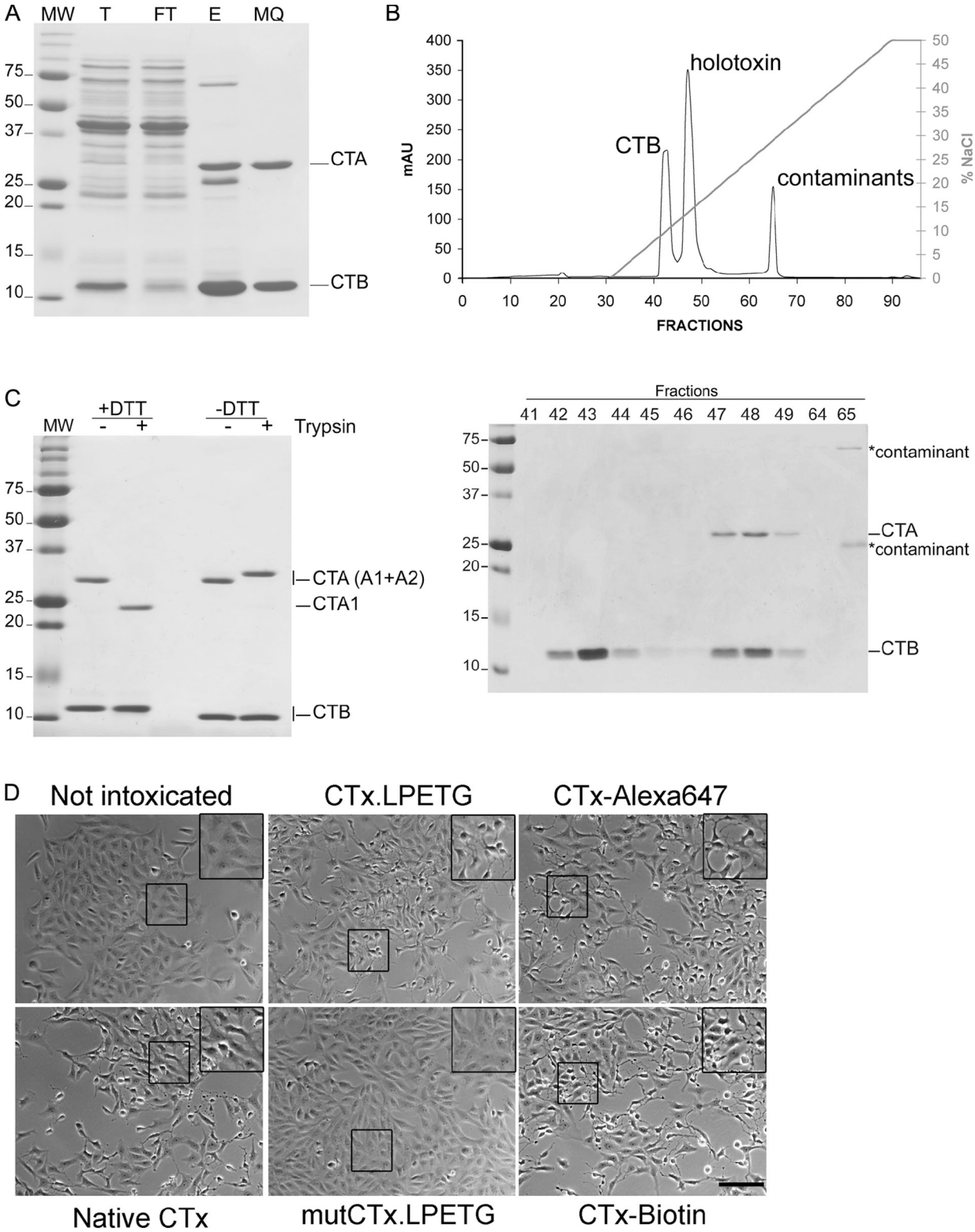

Figure 2. **Purification and characterization of CTx containing a sortase A recognition motif in the loop.** (A) CTx was expressed in *E. coli*. Lysed cells were centrifuged and the supernatant (lane T, equivalent of 200 µl of culture) was incubated with Ni-NTA agarose beads. The flow-through was discarded (lane FT, equivalent of 200 µl culture); the bound protein was eluted with imidazole (lane E, equivalent of 2 ml of culture) and further purified by ion-exchange chromatography (lane MQ, equivalent of 2 ml of culture). Lane MW shows molecular weight markers in kilodaltons. (B) Affinity chromatography profile for purification of the sortaggable CTx version: holocomplex (fractions 47–49), B pentamer only (fractions 40–44), and contaminants (fraction 65). (C) Purified CTx was incubated with trypsin or left untreated and analyzed under reducing and nonreducing conditions. All panels show SDS-PAGE gels stained with Coomassie. (D) Cellular toxicity assay for nonmodified CTx (*Native CTx*), wild-type, and inactive mutant (E110D/E112D) in the sortaggable version (*CTx.LPETG* and *mutCTx.LPETG*), and CTx labeled with Alexa Fluor 647 (CTx-Alexa 647) or biotin (CTx-biotin) at the C terminus of CTA1. Vero cells were intoxicated with 2 nM of the different versions of CTx for 2 h at 37°C. Phase-contrast images are shown. Insets on the top right corner show magnified views of the boxed regions. Bar, 100 µM.

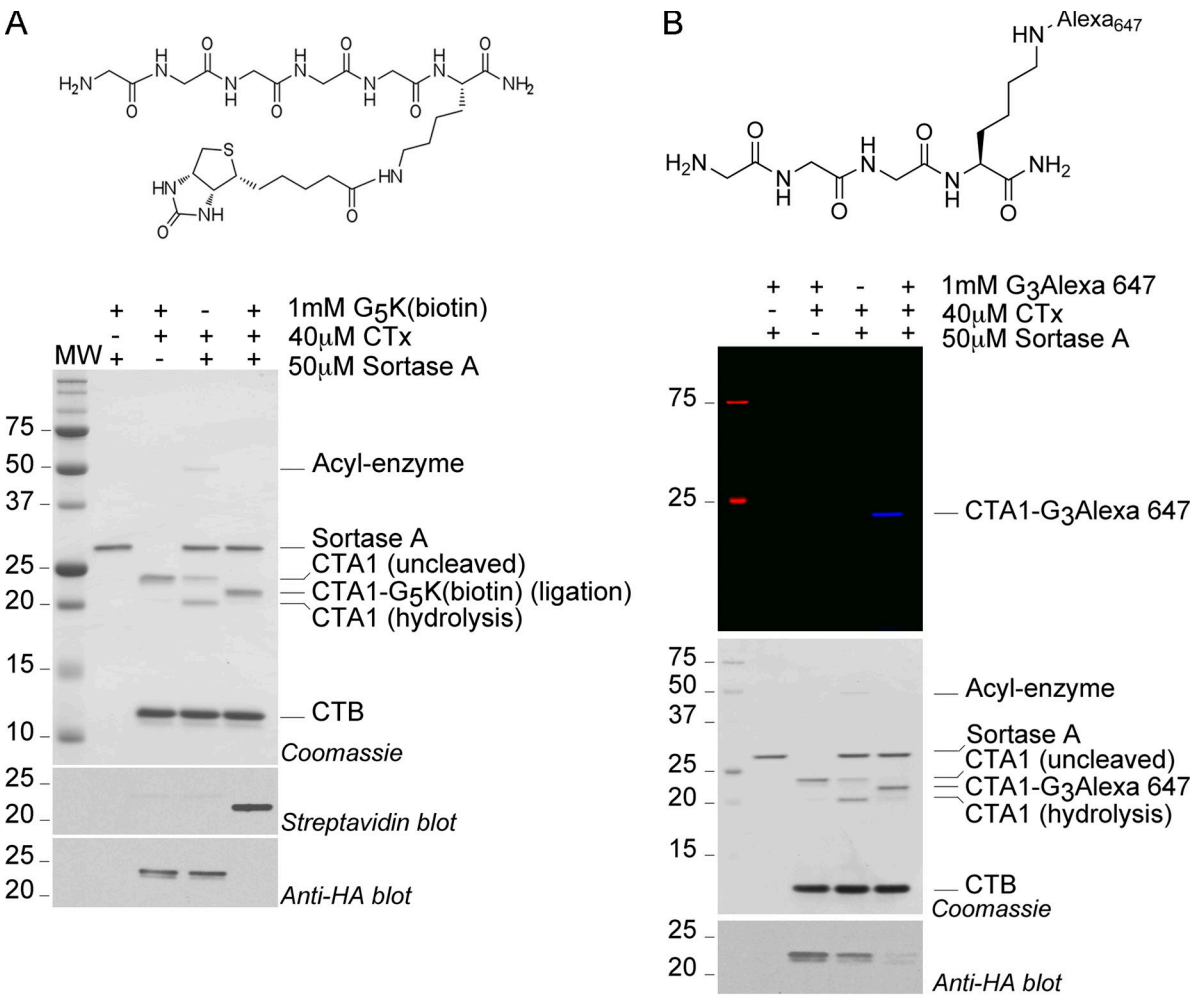

Figure 3. **Labeling of the C terminus of CTA1 with small peptides in the context of the preassembled holotoxin.** Purified sortaggable CTx was treated with trypsin and then incubated with sortase A in the presence of either a biotin-containing peptide (A) or an Alexa Fluor 647–containing peptide (B) as indicated. The structures of the corresponding peptides are shown in the top panels. Probes are appended to CTA1 quantitatively as assessed by Coomassie staining, fluorescence imaging, and streptavidin blotting, and by the loss of anti-HA immunoreactivity upon reaction (see text for details), as shown in the bottom panels. Lane MW shows molecular weight markers in kilodaltons.

To infer the maximum contribution of hydrolysis, we included a control reaction from which the oligoglycine peptide was omitted altogether. We show that near-quantitative (~95%) labeling of CTA1 is achieved with both biotin and fluorophores (Fig. 3, A and B, bottom). As expected, sortase A does not react with the B subunit of CTx (CTB) in these reactions, as the B subunit lacks a sortase A recognition motif. Both CTx-biotin and CTx-fluorophore are toxic even at low concentrations (Fig. 2 D).

At least 12% of the CTA1 pool that enters the cells traffics through the ER

Although it has been widely assumed that delivery and translocation of CTA1 across the ER is required for intoxication (Wernick et al., 2010b), the evidence on which the conclusion of ER involvement rests is for the most part indirect: it is based on pharmacological inhibition of trafficking by brefeldin A (Lencer et al., 1993; Nambiar et al., 1993; Orlandi et al., 1993), on the trafficking behavior of the B subunit (Fujinaga et al., 2003), or on in vitro experiments implicating ER-resident proteins in the dislocation of CTA1 (Schmitz et al., 2000; Tsai et al., 2001; Winkeler et al., 2003; Bernardi et al., 2008; Bernardi et al., 2010). Independent experimental approaches have failed to confirm some of these proposals (Saslowsky et al., 2010). Also, the ER retention signal at the C terminus of CTA is apparently not essential for intoxication, as disruption of the KDEL motif does not abolish toxicity (Lencer et al., 1995), unlike what is seen for *Pseudomonas aeruginosa* exotoxin A (Chaudhary et al., 1990).

To determine whether CTA1 indeed traffics through the ER in vivo, we used sortase to attach a bifunctional probe containing a biotin for specific detection of CTA1, and two consensus sites for N-linked glycosylation (only one of which would likely be used) to the C terminus of CTA1 (Fig. 4 A, G_3K(biotin)NNSTG). If CTA1 reaches the ER, then glycosylation should occur, provided the N-linked glycan attachment site is accessible to the glycosylation machinery. Genetic modification of toxins such as ricin with an N-glycosylation site to report on trafficking through the ER has been exploited before (Rapak et al., 1997).

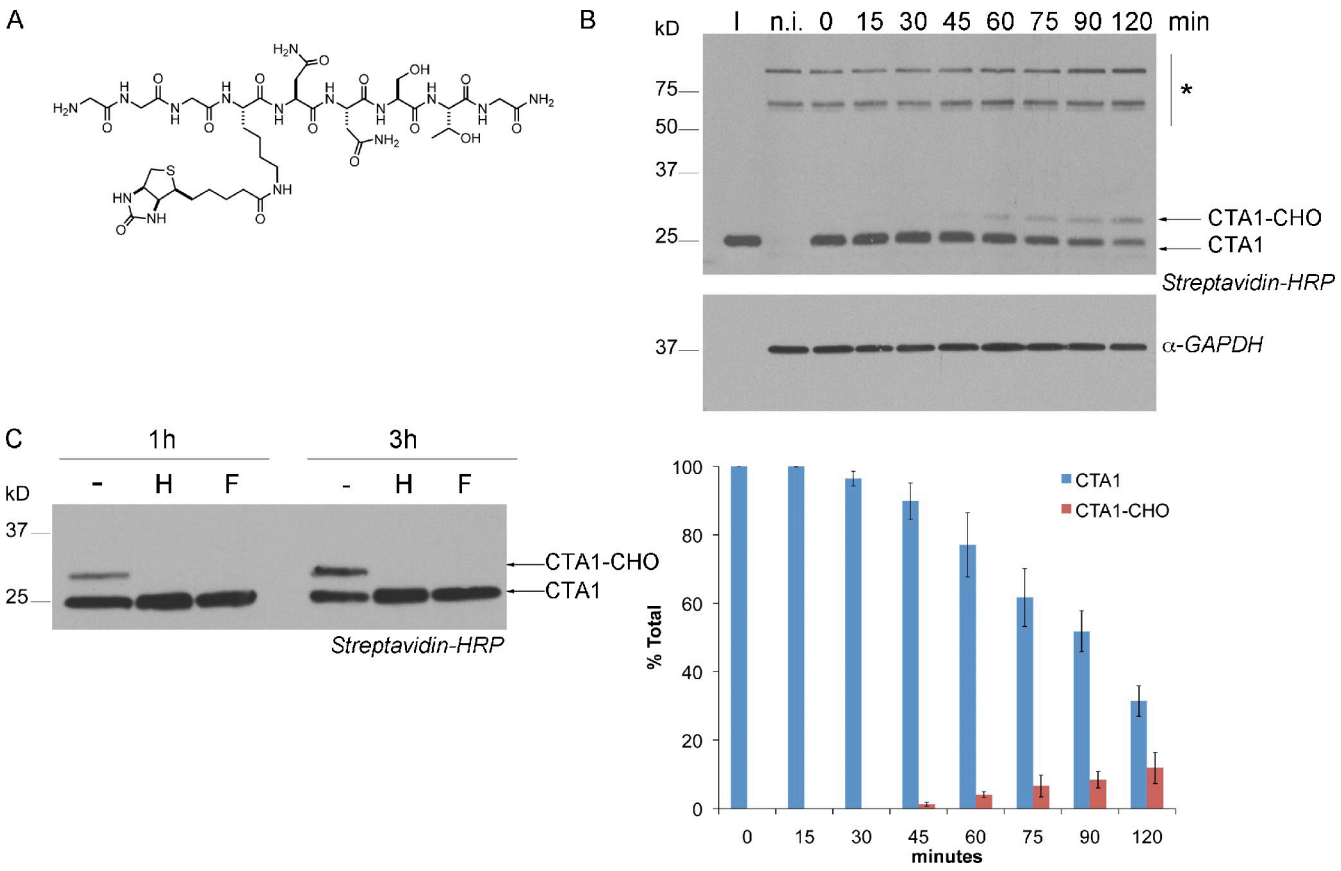

Figure 4. **A fraction of CTA1 that enters the cell traffics through the ER.** (A) Structure of the glycosylation reporter probe used. (B, top) Vero cells were intoxicated with CTx-G_3K(biotin)NNSTG. Glycosylation of modified CTx was followed in time by Streptavidin-HRP blotting on total cell lysates. GAPDH detected by immunoblotting was used as a loading control. Background biotinylated protein bands in the lysate are marker with an asterisk. (B, bottom) Quantification of the amount of CTx-G_3K(biotin)NNSTG that is glycosylated over time. The mean of three independent experiments ± SD is shown (error bars). The percentage of the total is defined as the ratio of either glycosylated or nonglycosylated forms of CTA1/levels of CTA1 at time point 0. (C) Vero cells intoxicated with CTx-G_3K(biotin)NNSTG were harvested at different time points and treated with Endo H (H) and PNGase F (F). CTA1-CHO is the N-glycosylated version of CTA1.

We monitored the fate of CTx-G_3K(biotin)NNSTG over time by immunoblotting analysis of total cell lysates using streptavidin-HRP. At 45 min after intoxication, we detected an electrophoretically distinct form of CTA1, the levels of which increased with time (Fig. 4 B, top). The apparent molecular mass difference of the two streptavidin-reactive CTA1 species is consistent with the acquisition of an ∼3-kD N-glycan, which suggests the use of a single N-glycosylation site. We confirmed the presence of an N-linked glycan by digestion with EndoH and PNGaseF (Fig. 4 C). At no time did we detect EndoH-resistant material, which showed that the high-mannose glycans attached to CTA1 were not converted into hybrid/complex-type N-linked oligosaccharides. We therefore conclude that CTA1, once glycosylated, does not enter the more distal portions of the secretory pathway, at least within the time frame of our experiment. Based on densitometric analysis, we estimate that a minimum of ∼12% of cell-bound CTA1-G_3K(biotin)NNSTG reaches the ER, as assessed by N-glycosylation (Fig. 4 B, bottom). Combined, these results show that sortase-mediated modifications at the C terminus of CTA1 are possible with retention of CTx quaternary structure, cell binding, and toxicity, and that the modified CTA1 reaches the ER.

Installation of a correctly folded protein at the C terminus of CTA1

The catalytic subunit of diphtheria toxin (DTA) recognizes diphthamide, a modified histidine residue in eukaryotic elongation factor 2 (eEF-2), ADP-ribosylates it to block protein synthesis, and so causes cell death (Collier, 2001; Liu et al., 2004). To kill cells, DTA needs to access the cytoplasm where diphthamide-modified eEF-2 is located. However, without its receptor-binding subunit, DTA fails to even enter the cell. Thus, if a fusion of CTx with DTA could mediate binding to cells and delivery of the DTA payload to the cytoplasm, toxicity should be observed. We could then use the CTx–DTA conjugate to perform a lethality-based genetic screen in human haploid cells to identify host factors essential for intoxication, as has been done for the native diphtheria toxin (DTx; Carette et al., 2009).

DTA (189 amino acids) is much larger than the short peptides tolerated as genetic fusions with CTx (21 amino acids; Wernick et al., 2010a), and therefore sortase-mediated reactions are an attractive alternative approach. We reasoned that a chemoenzymatic transformation of an already assembled holotoxin would overcome the issues associated with genetic extensions of CTA1, which have proven problematic exactly because they interfere with holotoxin assembly. To use DTA as a nucleophile

in these reactions, we expressed it recombinantly with an N-terminal hexahistidine handle for purification, followed by a thrombin cleavage site, and five glycines (His_6 LVPR^G_5DTA), a preparation readily purified by Ni-NTA and size exclusion chromatography. The His_6 LVPR^G_5DTA protein was cleaved with thrombin to remove the hexahistidine tag and so expose the required glycines at the N terminus (Antos et al., 2009). G_5DTA readily labels the C terminus of CTA1 in a sortase-catalyzed protein ligation reaction and does so with remarkable efficiency (>90%), based on the levels of conversion of CTA1 to CTA1-G_5DTA. Only in the reaction that contains all necessary components—sortase A, the sortaggable version of CTx, and the protein-based nucleophile—do we observe a polypeptide of the mass expected for a successful ligation (Fig. 5 A, *CTA1.G_5DTA*). "Sortaggable" CTx represents the sequence of CTx containing the sortase recognition motif LPETG installed in the CTA loop (Popp et al., 2007). The identity of the ligation product was confirmed by sequence analysis, including identification of the junction peptide between CTA1 and G_5DTA (Fig. 5 A and Fig. S2).

Using serial dilutions of the sortase reaction mixtures, we intoxicated KBM7 and Vero cells and measured their viability using a XTT colorimetric assay. We observed no cytotoxicity when CTx, sortase A, and G_5DTA were admixed but not covalently linked (Fig. 5 B, WtCTx + DTA and SortA + DTA). In contrast, cell death is detected only upon intoxication with the enzymatically prepared CTx–G_5DTA conjugate (Fig. 5 B, WtCTx − DTA). A similar effect (albeit showing slightly less toxicity) is observed using a nontoxic derivative of CTA1 (E110D/E112D) at the catalytic site (Fig. 5 B, *MutCTx-DTA*; Jobling and Holmes, 2000, 2001), which indicates that the observed toxicity indeed derives solely from the activity of DTA. Thus, the CTx–DTA conjugate is functional and indicates that CTx mediates transport of DTA from the plasma membrane to the cytoplasm.

Because CTx traffics through the endosomal/lysomal (E/L) system (Wernick et al., 2010b), toxicity of the CTx–DTA conjugate might result from the ability of DTA to cross E/L membranes into the cytoplasm (Collier, 2001) without having to be transported by CTA1, and with the role of CTx reduced to simply substituting for the receptor binding subunit of diphtheria toxin (DTx). Although we cannot formally exclude this possibility, the fact that we do not detect morphological alterations in Vero cells with the WtCTx–DTA conjugate in the presence of brefeldin A (+BFA, Fig. 5 C) suggests otherwise. BFA inhibits vesicular trafficking, causing redistribution of the Golgi apparatus and the trans-Golgi network (Fig. 5 C, Giantin panels, compare ±BFA; Doms et al., 1989; Lippincott-Schwartz et al., 1989), but it does not impair trafficking of DTA from the E/L system to the cytoplasm (Yoshida et al., 1991). Thus, if transport of the CTx–DTA conjugate to the cytoplasm was sustained by the DTA moiety, we should have detected morphological alterations in Vero cells even in the presence of BFA. This is not the case: we observe intoxication only in the absence of BFA (Fig. 5 C, compare CTx and CTx–DTA panels, ±BFA). In the short time frame of this experiment, no cellular morphological alterations or death were observed with DTx (Fig. 5 C, DTx panels), which indicates that any morphological alterations detected with CTx–DTA derive solely from the activity of CTx.

Human haploid genetic screens using the CTx-DTA conjugate

Based on our results, we hypothesize that DTA coupled to CTx traffics along the GM1 pathway (the receptor for CTx), an atypical route for DTA because the receptor for DTx is the heparin-binding EGF-like growth factor (Naglich et al., 1992). We further conclude that DTA is unable to exit from a compartment along the CTx intoxication route to the cytoplasm, unless assisted by CTA1 as its covalent fusion partner (Fig. 5 C). Dislocation of CTA1 would then be the rate-limiting step in delivering the DTA payload to the cytoplasm. A genetic screen performed with the CTx–DTA conjugate would thus identify genes involved in binding/trafficking of CTx from the plasma membrane to the cytoplasm, as well as genes involved in the biosynthetic pathway of diphthamide (the substrate for DTA). Genes encoding the cytosolic target substrates of CTA1 would not be found, as cells harboring mutations in those genes can still be killed by DTA.

We performed a genetic screen as described previously (Carette et al., 2011) using a pool of ∼100 million mutagenized haploid cells. Upon intoxication with the CTx–DTA conjugate, we expanded surviving cells, amplified the insertion sites, and subjected them to deep sequencing (Carette et al., 2011). We mapped the insertion sites to the human genome and identified those genes significantly enriched for disruptive mutations as compared with a control population of unselected mutagenized cells. This yielded seven candidate host factors with highly significant scores (P-values between 4×10^{-4} and 5×10^{-120}; Fig. 6 A and Tables S1 and S2). We identified *DPH2* and *WDR85*, genes involved in diphthamide biosynthesis and previously found in a haploid screen with DTx (Liu et al., 2004; Carette et al., 2009); ELF4, a member of the ETS family of transcription factors (Miyazaki et al., 1996), with its role in trafficking of CTx unknown; and *ST3GAL5*, *SLC35A2*, *B3GALT4*, and *UGCG*, genes whose products are involved in ganglioside biosynthesis (for review see Maccioni et al., 2011; Fig. 6 B), therefore affecting the levels of GM1 essential for binding of CTx to the cell. Using a fluorescently labeled version of CTx prepared via sortase-mediated reaction (CTx-Alexa647, Fig. 3 B), we show that CTx binds to *WDR85*-deficient cells but not to the *SLC35A2* mutant (Fig. 6 C, $WDR85^{GT}$ vs. $SLC35A2^{GT}$). However, toxin binding to the latter was readily restored by complementation with the respective cDNA (Fig. 6 C, SLC35A2 restored). We also observed binding of CTx-Alexa647 to a subset of *ST3GAL5* mutant cells. The same result was obtained in two independent clonal cell lines with gene trap insertions in the *ST3GAL5* locus (Fig. 6 C, $ST3GAL5^{GT\#1}$ and $ST3GAL5^{GT\#2}$). The existence of a mixed cell population (i.e., high- and low-binding CTx) was confirmed by flow cytometry. The majority of the *ST3GAL5*-deficient cells do not stain with CTx-Alexa647 (Fig. 6 D, ST3GAL5 low), but a minor fraction of cells (∼5–10%) bind CTx-Alexa647 at levels comparable to wild-type KBM7 cells (Fig. 6 D, ST3GAL5 high). To determine whether CTx binding to *ST3GAL5* cells could be the result of cross-contamination of cells or of partial

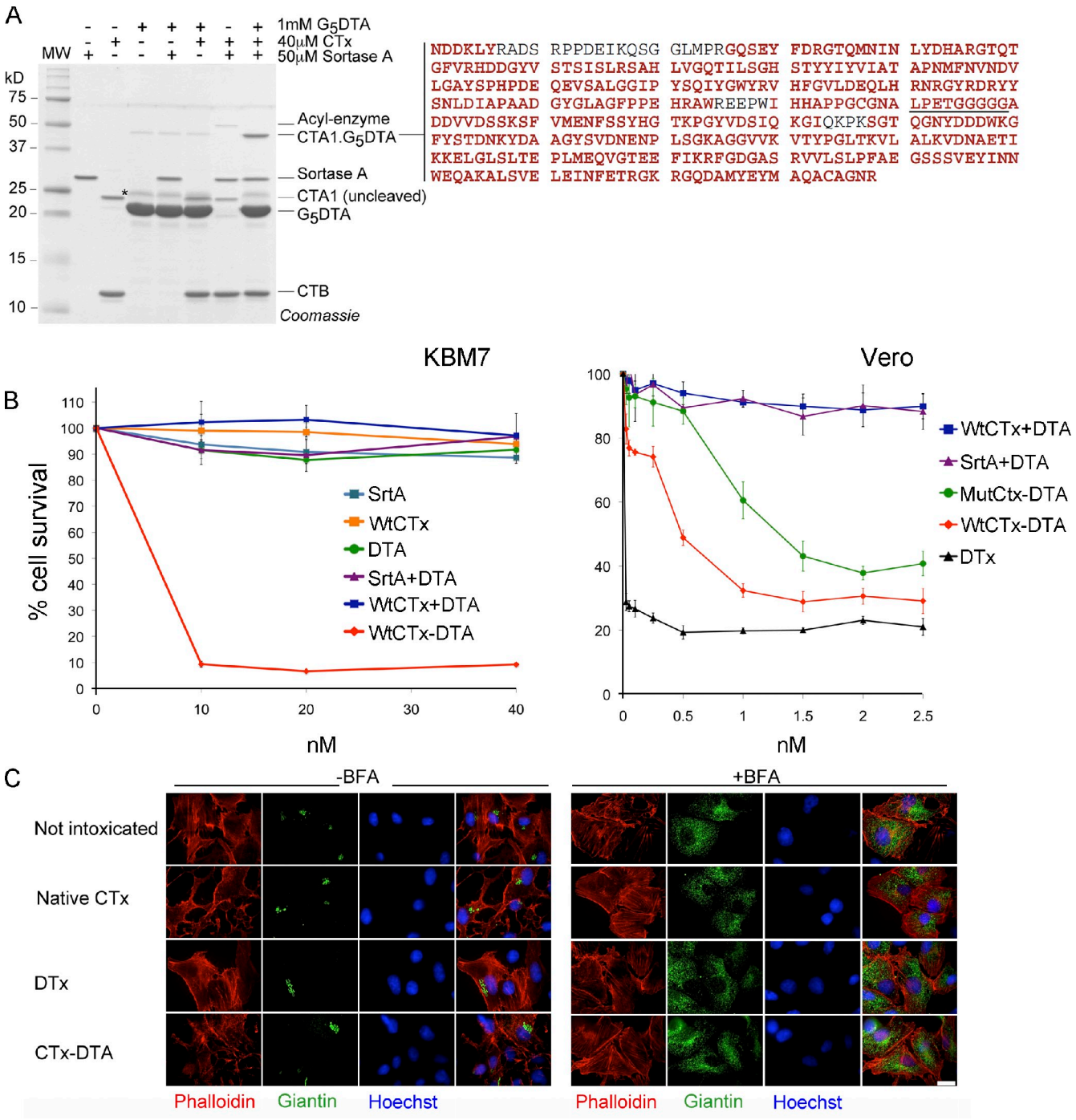

Figure 5. **Preparation and characterization of the Ctx–DTA conjugate.** (A) Attachment of the catalytic subunit of diphtheria toxin (G_5DTA) to the CTA1 chain of preassembled CTx holotoxin. The sortaggable version of CTx was incubated with sortase A in the presence and absence of G_5DTA (see text for details). G_5DTA is appended to CTA1 quantitatively as assessed by Coomassie staining. The identity of the polypeptide corresponding to CTA1-G_5DTA fusion was determined by electrospray ionization tandem mass spectrometry. The peptides identified are highlighted in red. The asterisk indicates a contaminant protein band in our DTA preparation. (B) Cytotoxicity of each of the sortase-mediated reactions shown in A was tested in KBM7 (left) and in Vero (right) cells. DTx corresponds to the native diphtheria holotoxin and is used as a positive control. Each data point represents the mean (n = 3) ± SD (error bars). "+" indicates separate addition of two unlinked molecules and "−" indicates covalent linkage of DTA to CTx. (C) Cytotoxicity of the CTx–DTA conjugate in Vero cells in the absence or presence of 100 ng/ml brefeldin A. Cells were intoxicated with 2 nM of each toxin for 2 h at 37°C, fixed, permeabilized, and stained with phalloidin, anti-giantin, and Hoechst. Note that the phalloidin staining changes only in the absence of BFA and when cells are intoxicated with either CTx or CTx–DTA. Bar, 10 μm.

reversion, we FACS sorted the two subpopulations (ST3GAL5 high and ST3GAL5 low) and performed RT-PCR analysis. *ST3GAL5* transcripts were absent from both samples (Fig. 6 E), showing that both clonal derivatives are true nulls for this gene. Different toxin-binding patterns thus do not arise from genetic variation but most probably result from different states of the clonal cells, for example because of cell cycle–dependent changes in receptor expression. When the FACS-sorted *ST3GAL5*

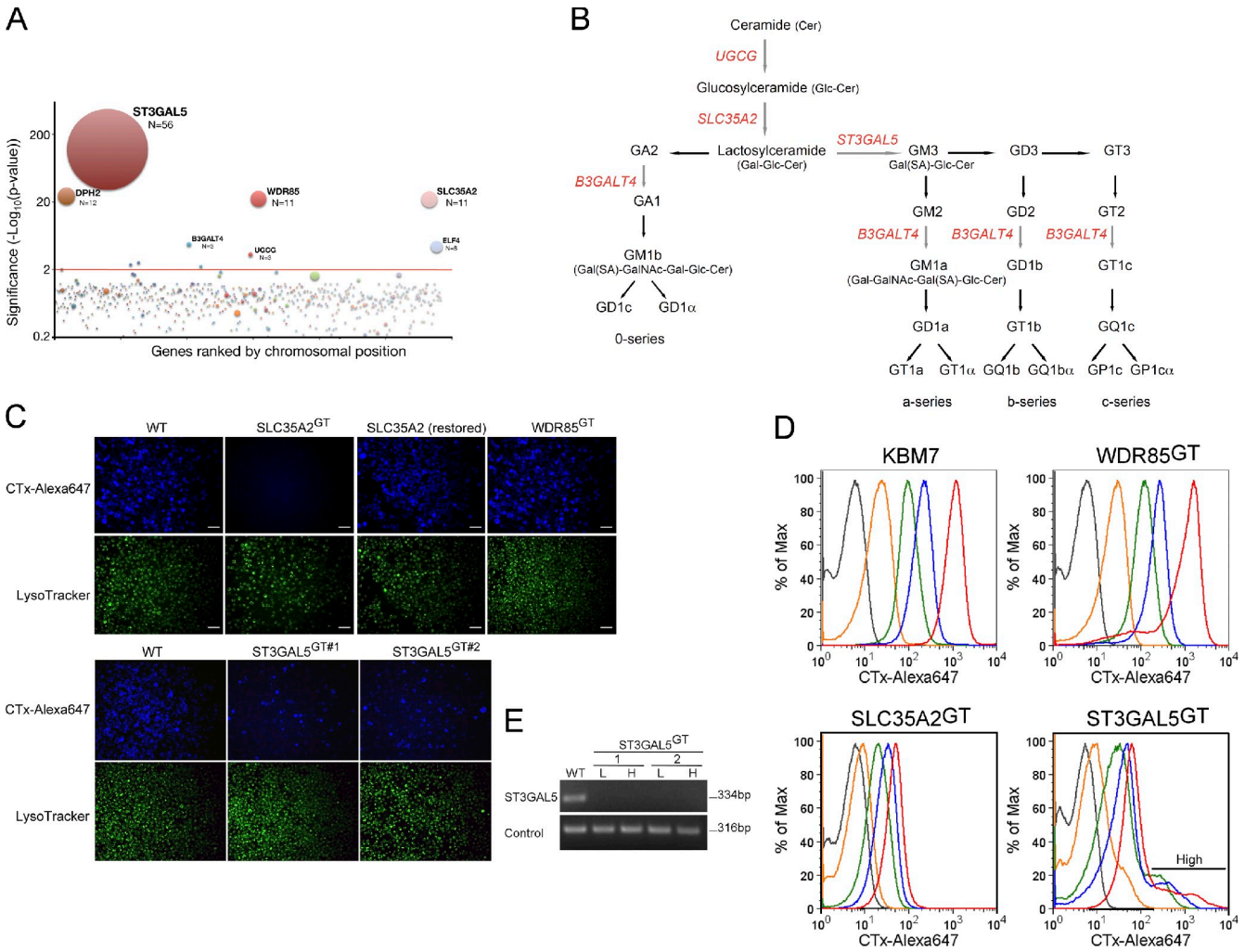

Figure 6. **Human haploid genetic screen using the CTx–DTA conjugate.** (A) Candidate host factors essential for intoxication by CTx–DTA as identified in the haploid genetic screen. Genes significantly enriched for gene-trap insertions in the CTx–DTA–selected cell population as compared with the nonselected mutagenized cell population. Circles represent genes and their sizes correspond with the number of independent insertions identified in the CTx–DTA selected cell population. Significantly enriched genes are labeled with gene names. Genes are ranked on the x axis based on their chromosomal location. N indicates the number of gene trap insertions found in each gene. (B) Representation of the ganglioside biosynthetic metabolic pathway indicating the essential genes identified in the CTx–DTA genetic screen. The figure was prepared based on data from Yamashita et al. (2003) and Maccioni et al. (2011). (C) CTx-Alexa647 and Lysotracker were added to mutant clonal cells identified in the genetic screen (*WDR85*^{GT}, *SLC35A2*^{GT}, and *ST3GAL5*^{GT}). *SLC35A2* mutant cells reconstituted with the respective defective cDNA (*SLC35A2 restored*) regain the ability to bind CTx. Bars, 10 µm. (D) Flow cytometry analysis of Alexa Fluor 647–positive cells upon intoxication of the different cell lines with various concentrations of CTx-Alexa647: 0, 0.2, 1, 2, and 10 nM (gray, orange, green, blue, and red, respectively) for 15 min on ice. The data shown are representative of independent experiments. (E) The low (L) and high (H) CTx-Alexa647 binding populations of ST3GAL5 were FACS sorted, and total RNA was isolated. RT-PCR analysis showed undetectable *ST3GAL5* mRNA levels in two independent clonal cells containing gene trap insertions in the *ST3GAL5* locus.

subpopulations were cultured to obtain yet new clonal derivatives, again a mixture of high- and low-binding CTx subpopulations was obtained (unpublished data). Differential binding of CTx-Alexa647 to the *ST3GAL5* mutant cells may reflect cell cycle–dependent variation in the levels of GM1b ganglioside from the 0 series, the synthesis of which is independent of the activity of GM3 synthase (Fig. 6 B; Yamashita et al., 2003; Simpson et al., 2004), as discussed below.

Discussion

Haploid genetic screens using human KBM7 cells have allowed identification of host factors essential for intoxication by different cytolethal bacterial toxins (Carette et al., 2011). CTx does not kill KBM7 cells, which precludes the use of such screens to identify host factors for CTx trafficking. We overcame this problem by attaching a toxic warhead to CTA1 in the context of the CTx holotoxin, thus converting it into a lethal entity. Because a genetic screen had been conducted with native DTx (Carette et al., 2009), we chose to conjugate its toxic subunit DTA to CTx, so a comparison of hits obtained in both screens (i.e., DTx and CTx–DTA) would allow an unambiguous assignment of genes that specifically contribute to binding and/or trafficking of CTx.

Successful installation of protein-sized moieties such as GFP by genetic fusion with CTA1 in the context of the holotoxin has never been reported, and genetic fusion of a short sequence to the N terminus of CTA1 lead to rapid degradation

of the modified subunit (Wernick et al., 2010a). Thus, to be able to modify the C terminus of CTA1 in the context of a preassembled holotoxin, we developed sortase-mediated reactions. Sortase recognizes a five–amino acid motif, which we placed in the loop that connects CTA1 and CTA2, with preservation of the intrachain disulfide bond present in the CTA precursor. Optimal conversion of CTA1 into labeled CTA1 requires prior nicking of this loop with trypsin to fully expose the sortase recognition motif. We first validated the sortase-based labeling method using biotin and fluorophore-containing peptides to demonstrate that transformations at the C terminus of CTA1 are possible without compromising CTx quaternary structure, receptor binding, and entry. The sortase recognition motif, the installation of biotin, and the installation of Alexa Fluor 647 at the C terminus of CTA1: none of these compromise toxicity of CTx as inferred from the morphological changes elicited by the modified toxins.

Using sortase to attach a biotinylated N-linked glycosylation reporter peptide to the C terminus of CTA1 in the context of the holotoxin, we could show arrival of CTA1 in the ER. Previous evidence for delivery of CTA1 to the ER came from experiments using a genetically engineered CTB subunit with a glycosylation recognition motif, but only a minor fraction of CTA1 was immunoprecipitated along with glycosylated and therefore ER-resident CTB (Fujinaga et al., 2003). Because the intracellular distribution of oxidoreductases is not confined to the ER (Arunachalam et al., 2000), if reduction of the disulfide bond that links CTA1 and CTA2 had occurred in other subcellular compartments, then CTA1 could have trafficked independently of CTB for intoxication to occur. Also, glycosylated CTB could have re-associated with free CTA1 upon lysis of intoxicated cells. Here we estimate that at least 12% of the fraction that enters the cells engages the host glycosylation machinery in the ER. This is a minimum estimate, as the efficiency of glycosylation of the modified CTA1-GGGK(biotin)NNSTG may fall well short of completeness.

Having established conditions to modify CTx using sortase, and having shown that the modified versions retained key features of native CTx, we attached the far more bulky catalytic subunit of diphtheria toxin, DTA, to CTA1. The resultant conjugate was cytotoxic to both Vero and KBM7 cells and could therefore be used to perform a genetic screen in KBM7. It is the CTx portion that must dictate trafficking of CTx–DTA because brefeldin A has a protective effect toward CTx–DTA, but not toward diphtheria holotoxin activity (Yoshida et al., 1991). This suggests that the mechanisms used by CTA1 to reach the cytoplasm involve components that can accommodate passage of even a modestly sized protein like DTA (21 kD, about the same as that of CTA1 itself) when covalently attached to CTA1.

The CTx–DTA conjugate was then used to perform a genetic screen in KBM7 cells (Carette et al., 2009; Carette et al., 2011). Among the identified hits were proteins involved in the synthesis of diphthamide (the substrate for DTA and hence entirely expected) and gangliosides (the entry factor for CTx). Although 98% of the expressed genes carry insertions in the pool of mutants that serves as the starting population for our genome-wide screen (Carette et al., 2011), no ER-resident or cytoplasmic proteins that could obviously participate in the transport of CTA1 from a subcellular compartment to the cytoplasm were identified. We offer four explanations to account for this observation: first, our screen may not have reached saturation, a possibility supported by the absence of mutants in other genes (*DPH1* and *DPH5*) known to be involved in diphthamide synthesis, even though we have shown that such genes can be successfully targeted in this approach (Carette et al., 2009). Second, genes involved in the dislocation of CTA1 may be essential for cell survival, and therefore cells carrying disruptive gene-trap insertions in such genes may be purged from the mutagenized pool of cells used to conduct the genetic screen. Third, the CTx–DTA conjugate might reach the cytosol using a trafficking route that is not usually exploited by CTA1. Although in the presence of BFA the typical morphological alterations of intoxication by CTx are not detected (Fig. 5 C), it is still possible that a minor fraction of CTA1–DTA, sufficient to kill the cell, reaches the cytosol and thus eliminates cells mutant in genes normally important for intoxication by CTx. Fourth, CTA1 might reach the cytoplasm using more than one pathway. Whether endosomal and/or Golgi compartments are competent to allow egress of CTx is open to debate. Escape from compartments other than the ER could explain why a mutation in the C-terminal KDEL retrieval signal of CTA does not eliminate toxicity of CTx (Lencer et al., 1995), whereas for the ADP-ribosylating *P. aeruginosa* exotoxin A, the homologous ER retrieval signal is essential for intoxication (Chaudhary et al., 1990). Also, redundant pathways may support intoxication by CTx: if a main route is blocked by mutation of a key component, an alternative route may still be used. Deficiency in proteins involved in dislocation of misfolded proteins is compensated by adjustments in the expression of other components: members of the Derlin-nucleated dislocation complex—Sel1L, Hrd1, OS9, and Ubc6e—are all up-regulated in response to the complete absence of Derlin-2 (Dougan et al., 2011). Although involvement of Derlin-1 in dislocation of CTA1 has been claimed (Bernardi et al., 2008; Dixit et al., 2008), it was not confirmed in a recent screen performed in zebrafish embryos (Saslowsky et al., 2010). Instead, the latter approach pointed to flotillin-1 and flotillin-2 as protein players in trafficking of CTx. Neither of these proteins was identified in our genetic screen, most probably because flotillin mutant cells do not confer complete resistance to CTx (Saslowsky et al., 2010). The same holds true for torsinA, an ER membrane protein recently implicated in dislocation of CTA1 (Nery et al., 2011). Any fotillin- or torsinA-deficient cells would have been purged from the mutant pool over the intoxication period of time required to select a manageable population of surviving resistant cells.

Our genome-wide strategy positively identified genes involved in the synthesis of gangliosides as essential for intoxication by CTx. The assigned receptor for CTx is the ganglioside GM1, and so identification of *UGCG* and *SLC35A2* is in line with expectations, as disruption in either one of these genes impairs the synthesis of lactosylceramide, the precursor of the entire series of gangliosides. Identification of the *B3GALT4* gene was also expected, as it encodes GM1 synthase, which catalyzes the synthesis of both GM1a and GM1b gangliosides

(Maglione et al., 2010; Maccioni et al., 2011). In contrast, implication of the *ST3GAL5* gene in CTx intoxication was unexpected and adds a new twist to our understanding of ganglioside biosynthesis in its relation to CTx intoxication. The *ST3GAL5* gene product is involved in the synthesis of GM3, which is not only a precursor for GM1a but also for most of the more complex ganglioside lipids (Yamashita et al., 2003; Simpson et al., 2004). Knockout of *ST3GAL5* in mouse embryonic fibroblasts activates an alternative biosynthetic pathway of gangliosides from the 0 series (Shevchuk et al., 2007). Therefore synthesis of GM1a, but not of GM1b, is impaired in these cells. Paradoxically, no gangliosides from the 0 series were detected by thin-layer chromatography in human skin fibroblasts derived from patients with point mutations in the *ST3GAL5* gene, which suggests that no alternative synthetic pathway of gangliosides exists in these cells (Liu et al., 2008). Whether CTx is able to intoxicate mouse and/or human GM3-synthase–deficient fibroblasts remains to be determined, but our work shows that human *ST3GAL5*-null cells are resistant to intoxication by CTx. Thus, either gangliosides from the 0 series are not synthesized by these cells, or if GM1b is being synthesized, it is not sufficient to deliver CTx to its target destination.

We isolated the *SLC35A2* and *ST3GAL5* mutant cells from our selected pool of cells, and using Alexa Fluor 647–conjugated CTx, we showed that toxin binding is compromised in both cell types. However, in the particular case of *ST3GAL5*, we identified a subset of *ST3GAL5*-null cells that supports CTx binding at levels comparable to wild-type cells. Because differential expression of glycosphingolipids at the plasma membrane is cell cycle dependent (Majoul et al., 2002), we speculate that the *ST3GAL5*-null cells have an alternate, possibly cell cycle–specific 0 pathway for ganglioside synthesis.

The mutant cells identified in our genetic screen are useful tools not only to address the physiological roles of gangliosides in human cells but also to dissect binding and trafficking of other pathogens and their products. Their retrieval was possible through the generation of a cytolethal version of CTx, which then enabled us to conduct the genetic screen in haploid cells. Chemical mutagenesis in diploid CHO cells has been used to generate CTx-resistant clones (Teter and Holmes, 2002), but in this case, the identity of the mutant genes that confer resistance is unknown and would be difficult to establish. Almost certainly, such chemically mutagenized cells carry mutations in many genes irrelevant for the phenotype selected for, and only a complementation test would provide a clue to the nature of the mutation. In contrast, our genetic screen in human haploid cells yields mutants with defined lesions, readily restored to wild-type phenotype by provision of the corresponding cDNAs, as shown here for *SLC35A2*.

Based on the ease and versatility of sortase-mediated reactions, we envision that the sortase-labeling platform described for CTx can be applied to other toxins that display either an exposed cleavable loop or an exposed C terminus, such as heat labile enterotoxin (Sixma et al., 1991), shiga toxin (Fraser et al., 1994), exotoxin A (Allured et al., 1986), and cytolethal distending toxins (Nesić et al., 2004). The combination of modified toxins with a robust genetic screening approach, as described here, can extend the range of tools to address intracellular trafficking more generally.

Materials and methods

Cloning and expression of the sortaggable version of CTx

The LPETG.G.HA sequence was introduced into the loop of CTA1 using a QuikChange II site-directed mutagenesis kit (Agilent Technologies) and the following oligonucleotides: 5′-GGTTGTGGGAATGCTCTTCCTGAGACCG-GTGGTTACCCATACGATGTT-3′ and its reverse-complement counterpart. The template used was a bi-cistronic arabinose-inducible pARCT plasmid encoding CTA and CTB proteins with the corresponding signal peptides of the *E. coli* heat-labile enterotoxin II subunits (a gift from W. Lencer, Children's Hospital Boston, Harvard Medical School, Boston, MA). The inactive mutant E110D/E112D was created by site-directed mutagenesis using the following oligonucleotides: 5′-AGTCCTCATCCAGATGACCAAGAC-GTTTCTGCTTTAGGTGG-3′ and its reverse-complement counterpart. The template used was the plasmid encoding the sortaggable version of CTx. A single protocol for expression and purification of the different CTx versions was used. In brief, the various constructs were transformed into the *E. coli* BL21strain (Promega). A stationary phase starter culture prepared in sterile lysogeny broth (LB) media supplemented with 35 µg/ml chloramphenicol was diluted 50 times with freshly prepared nonautoclaved Terrific Broth media (Sigma-Aldrich) supplemented with chloramphenicol. At mid-log phase, expression of CTA and CTB proteins was induced with 0.25% (wt/vol) arabinose (Sigma-Aldrich) for 3 h at 37°C. Cells were harvested and resuspended in 50 mM Tris-Cl, 300 mM NaCl, and 1 µg/ml polymixin B (Sigma-Aldrich), pH 8.0, supplemented with protease cocktail inhibitors (Roche). The suspension was stirred at 25°C for 30 min and centrifuged at 10,000 *g*. The supernatant was incubated with Ni-NTA agarose (QIAGEN; 0.25-ml bed volume per 1 liter culture) for 30 min at 25°C. The resin was washed with 20 column volumes of 50 mM Tris-Cl and 300 mM NaCl, pH 8.0, and the protein was eluted with 20 mM Tris-Cl, 150 mM NaCl, and 300 mM imidazole, pH 8.0. CTx was further purified by anion-exchange chromatography on a Mono-Q column (GE Healthcare) and eluted using a linear salt gradient generated with 20 mM Tris-Cl, pH 8.0, 20 mM Tris-Cl, and 1 M NaCl, pH 8.0. Fractions containing the holotoxin were analyzed by SDS-PAGE and Coomassie staining, pooled, and concentrated. 10% glycerol was then added. The protein preparation was aliquoted, snap frozen, and stored at −80°C. The protein concentration was determined by Bradford Assay (Bio-Rad Laboratories).

Synthesis of GGGK-Alexa647 and GGGK(biotin)NNSTG

The GGGK peptide was synthesized manually by standard Fmoc-based solid-phase peptide synthesis protocols on Rink Amide resin (Novabiochem; EMD). The Fmoc-protected peptide was cleaved from the resin by treatment with 2.5 mL of 95:3:2 TFA/TIPS/H_2O (5×, 15 min each) that also removed the 4-methyltrityl (Mtt) protecting group on the lysine residue. The combined cleavage solutions were concentrated, dissolved in methanol, and precipitated with cold diethyl ether. Coupling of the Fmoc-protected peptide to the amine-reactive Alexa Fluor dye was accomplished in solution. One equivalent of Fmoc-GGGK peptide was mixed with 0.5 equivalents of Alexa Fluor 647 carboxylic acid, succinimidyl ester (Invitrogen), and four equivalents of *N*,*N*-Diisopropylethylamine (Sigma-Aldrich) in anhydrous DMSO, then incubated at room temperature for 6 h. Under these conditions, Fmoc deprotection also occurred. The Alexa Fluor 647 peptide was purified on a 5PE column (8 × 250 mm, MeCN/H_2O gradient mobile phase with 0.1% TFA, 3 mL/min; Waters). We were unable to observe the Alexa Fluor 647 peptide with a matrix-assisted laser desorption/ionization time-of-flight mass spectrometer, so we inferred the molecular weight and activity as a nucleophile by setting up a test transpeptidation reaction with sortase A and an LPETG-tagged GFP substrate as described previously (Popp et al., 2007), then observing the mass change in the transpeptidation product by electrospray ionization mass spectrometry on a liquid chromatography mass spectrometer (Micromass MS Technologies), an HPLC system equipped with an HTC PAL autosampler (Paradigm MG4; Michrom BioResources), and a Symmetry 5 mm C8 column (2.1 × 50 mm, MeCN/H2O (0.1% formic acid) gradient mobile phase, 150 ml/min; Waters). The predicted molecular weight for the Alexa Fluor 647 peptide is 1,155.06 g/mol, obs = 1155.0 g/mol. The GGGK(biotin)NNSTG peptide was synthesized using standard solid phase peptide synthesis.

Cloning and expression of G_5DTA

The construct pET-15b encoding an LFN-DTA fusion protein was used as a template (Addgene 11075; Milne et al., 1995). This plasmid was first digested with NcoI to remove the LFN sequence, and the five glycines were introduced at the N terminus of DTA by site-directed mutagenesis using the following oligonucleotides: 5′-CTGGTTCCACGTGGTGGAGGTGGAGGTGCTGACGACGTTGTT-3′ and its reverse-complement counterpart. The His_6 LVPR^G_5DTA protein was expressed in *E. coli* BL21(DE3). Cells were grown in LB containing 200 µg/ml ampicillin to mid-log phase. Protein expression was induced with 1 mM IPTG for 3 h at 37°C and cells were harvested by centrifugation. The cell pellet was resuspended in 50 mM Tris-Cl, 150 mM NaCl, and 20 mM imidazole, pH 8.0, supplemented with protease cocktail inhibitors, lysed by French press, and centrifuged. The cleared lysate was then applied to a Ni-NTA column equilibrated with 50 mM Tris-Cl, 150 mM NaCl, and 20 mM imidazole, pH 8.0. The column was washed with 20 column volumes of buffer and the protein was eluted with 50 mM Tris-Cl, 150 mM NaCl, and 300 mM imidazole, pH 8.0. The buffer was exchanged to 20 mM Tris-Cl and 150 mM NaCl, pH 8.0, using a desalting column (PD10 Sephadex; GE Healthcare). The material was concentrated to 1 ml using centrifugal concentrators (Vivapsin 500; Sigma-Aldrich) and subjected to thrombin cleavage (Thrombin CleanCleave Kit; Sigma-Aldrich) for 16 h at 25°C. Cleavage was monitored by SDS-PAGE followed by Coomassie staining upon which the reaction was filtered to remove the thrombin beads. G_5DTA was further purified by size exclusion chromatography on a HiLoad 16/60 Superdex 75 column (GE Healthcare), eluting with 50 mM Tris-Cl, 150 mM NaCl, and 10% glycerol (wt/vol), pH 8.0, at a flow rate of 1 ml/min. Fractions containing G_5DTA were pooled, concentrated, aliquoted, and stored at −80°C. Protein concentration was estimated by UV-visible spectroscopy using the absorbance of G_5DTA at 280 nM (calculated extinction coefficient 25,900 M/cm).

Sortase-labeling reactions

Sortase A_{Staph} was expressed and purified as described previously (Popp et al., 2007). In brief, sortase A_{Staph} (residues 26–206) containing an N-terminal His_6 tag was expressed in *E. coli* BL21(DE3). Cells were grown in LB containing 0.1 mg/ml ampicillin to an optical density of 0.6 at 600 nm. Protein expression was induced with 1 mM IPTG for 3 h at 37°C. Cells were harvested by centrifugation, and the pellet was resuspended in 50 mM Tris-Cl, 150 mM NaCl, and 10 mM imidazole, pH 8.0, supplemented with protease cocktail inhibitors, then lysed a by French press and centrifuged. The cleared lysate was then applied to a Ni-NTA column previously equilibrated with the resuspension buffer. The column was washed with 20 column volumes of 50 mM Tris-Cl, 150 mM NaCl, and 10 mM imidazole, pH 8.0. The protein was eluted with 5 column volumes of 50 mM Tris-Cl, 150 mM NaCl, and 300 mM imidazole, pH 8.0. The buffer was exchanged to 20 mM Tris-Cl, 150 mM NaCl, and 10% glycerol, pH 8.0, using a desalting column (PD10 Sephadex). Protein concentration was estimated with a Bradford assay. The purified protein was concentrated to a 0.6-mM stock solution, aliquoted, and stored at −80°C until further use.

Before a sortase reaction, the engineered sortaggable loop of cholera toxin was cleaved with immobilized trypsin (Thermo Fisher Scientific) at 25°C for 90 min (2 µl of a 50% slurry per 200 µg of protein). Cleavage was monitored by SDS-PAGE under reducing conditions. Upon complete cleavage of the loop, trypsin beads were removed by filtration. Typical sortase reactions contained 40 µM CTx, 50 µM sortase A, and 1 mM nucleophile in sortase buffer (50 mM Tris-Cl, 150 mM NaCl, and 10 mM $CaCl_2$). The reactions were incubated at 37°C for 5 h (when using small probes) or at 25°C for 16 h (when using proteins as nucleophiles). The reaction buffer was exchanged to PBS containing no $CaCl_2$ using a NAP Sephadex column (GE Healthcare). This step starkly reduces sortase activity, which is calcium dependent, and also allows removal of excess free peptide. The final preparations were stable at 4°C for at least 2 wk. Although high ligation yields are achieved using the conditions described, the CTx–G_5DTA conjugate used to intoxicate Vero cells in Fig. 5 C was further purified by size exclusion chromatography as described for G_5DTA. Fractions containing pure CTx–G_5DTA were pooled, concentrated, and aliquoted, and the protein concentration was determined with a Bradford assay.

Cell proliferation assay

Cells were treated continuously for 16 h at 37°C in a 5% CO_2 atmosphere with different amounts of the various toxins and controls as indicated in the legend to Fig. 5.

Cell viability was determined using the XTT cell proliferation kit from Roche according to the manufacturer's instructions.

Genetic screen in KBM7 cells and isolation of the mutant clones

The genetic screen with the CTx–DTA conjugate was performed on 100 million mutagenized KBM7 cells (Carette et al., 2011). Cells were exposed to 1.5 mg CTx–DTA for 2 wk before harvesting the survivors. Analysis of the screen was performed essentially as described previously (Carette et al., 2011). In brief, the sequences flanking retroviral insertion sites were mapped on the human genome (Table S1) using inverse PCR followed by Illumina sequencing. The number of inactivating mutations (i.e., sense orientation or present in exon) per individual gene was counted as well as the total number of inactivating insertions for all genes. Enrichment of a gene in the CTx–DTA–treated population was calculated by comparing how often that gene was mutated in the population with how often the gene carries an insertion in the untreated control dataset. For each gene, a P-value (corrected for false discovery rate) was calculated using the one-sided Fisher exact test (Table S2). Both *WDR85* and *SLC35A2* gene hits had already been identified in previous genetic screens with diphtheria toxin and influenza virus, respectively (Carette et al., 2009), and clonal cells defective in these genes were therefore available. To retrieve the *ST3GAL5* mutant cells, we FACS sorted individual cells from the pool resistant to intoxication by CTx–DTA. Cells were grown until confluent in Iscove's modified Dulbecco's medium media supplemented with 10% inactivated fetal calf serum and penicillin/streptomycin at 37°C in a 5% CO_2 atmosphere. Genomic DNA was then extracted from the different individual cell lines using the QiaAmp DNA mini kit (QIAGEN) according to the manufacturer's instructions. The presence of a gene trap within the *ST3GAL5* gene in any of the isolated cell lines was determined by PCR using a forward primer located within the gene trap (5′-CTCGGTGGAACCTCCAAAT-3′) and a reverse primer designed to target the ST3GAL5 gene (5′-CACACTTCCTCTGCTGCAGTA-3′). Two positive clones were identified and the gene trap insertions were mapped by direct sequencing of the PCR product using the forward primer. Absence of the *ST3GAL5* transcript in the isolated mutant cells was determined by RT-PCR. Total RNA was extracted from both the KBM7 and *ST3GAL5* mutant cells using the RNeasy Mini kit (QIAGEN). cDNA was synthesized using 1 µg of total RNA from each sample with the SuperScriptTM III First-Strand synthesis system for RT-PCR (Invitrogen). Amplification of *ST3GAL5* was performed using the following primers: 5′-GCCGAGCAATGCCAAGTGAG-3′ and 5′-CAGCGCCATTGATGTCTTGG-3′. Amplification of *SLC35A2* was used as a control and performed using the following primers: 5′-CTCACAGGCGCCTGAAGTAC-3′ and 5′-GGAAAGTGGCAGCTGGTAG-3′.

Microscopy experiments and image acquisition

Toxicity of the various versions of CTx was determined in Vero cells. In Fig. 2, cells were grown until 85% confluence in a 24-well plate and then intoxicated for 2 h at 37°C with 2 nM CTx (either native or modified as indicated). Imaging was performed at room temperature on an inverted microscope (Eclipse TE2000-E; Nikon) using a 10× magnification lens (Nikon) and a 1× NA. In Fig. 5, Vero cells were treated with 100 ng/ml brefeldin A for 1 h before intoxication. Cells were then fixed with 4% paraformaldehyde in PBS, permeabilized with 0.1% Triton X-100 in PBS, and stained with an antibody directed to giantin (Abcam), phalloidin, and Hoechst (Invitrogen). In Fig. 6, binding of CTx to KBM7 and to the various mutant cell lines was tested by incubating the cells with 20 nM CTx-Alexa647 (prepared as described earlier in Materials and methods) and LysoTracker Red (Invitrogen) at 37°C for 10 min. Cells were washed with PBS, resuspended in Opti-MEM media (Invitrogen), and plated onto poly-L-lysine L–coated microscopy slides (Polysciences, Inc.). Images were acquired at 37°C using a spinning disk confocal microscope (TE2000-U; Nikon) and a 3-W water-cooled laser with an acoustic-optic tunable filter (Prairie Technologies), 20× magnification, and a 1.4× NA. An Orca ER camera (C4742-95-12ERG; Hamamatsu Photonics) and MetaMorph software (Molecular Devices) were used for acquisition.

Flow cytometry analysis

FACS assays were performed with the inactive mutant of CTx (E110D/E112D) conjugated to GGGK-Alexa647 at its CTA1 using sortase as described earlier in Materials and methods. Cells were incubated for 15 min on ice with CTx-Alexa647 and propidium iodide (PI), washed with cold PBS supplemented with 1% fetal bovine serum, and submitted to FACS analysis immediately (FACS Calibur; BD). Control samples were prepared using PI only. Only cells negative for PI staining were gated for data acquisition. FlowJo was used to analyze the data. Intensity of fluorescence was measured and the percentage maximum is presented in the overlaid histograms.

Glycosylation assay

Vero cells (85% confluent in a 10-cm dish) were trypsinized with 0.05% Trypsin-EDTA and harvested by centrifugation. Upon washing with PBS, the cells were resuspended in 100 µl of Opti-MEM media and intoxicated with CTx-G_3K(biotin)NNSTG at a final concentration of 20 nM on ice for 10 min. The cells were then diluted in 10 ml Opti-MEM and incubated at 37°C. 1-ml aliquots were taken at the indicated time points. The cells were sedimented, washed with PBS, and snap frozen. For SDS-PAGE, the cells were thawed on ice and lysed in 0.1% SDS (vol/vol) in 50 mM Tris-Cl, pH 8.0, in the presence of 0.5 mg/ml PMSF. Protein concentration was determined with a bicinchoninic acid assay (Thermo Fisher Scientific), and equal amounts of total protein were loaded onto a 10% SDS-PAGE gel. The biotinylated CTx was visualized by immunoblotting using a streptavidin–HRP conjugate and ECL detection substrates. The film was scanned and the bands were quantified using the public-domain ImageJ program (National Institutes of Health).

Digestion with Endoglycosidase H and PNGase F (New England Biolabs, Inc.) was performed at 37°C for 1 h after retrieval of biotinylated CTx species from the cell lysates using streptavidin beads (Sigma-Aldrich).

Miscellaneous

Fluorescent gel images were obtained using a variable mode imager (Typhoon 9200; GE Healthcare). For mass-spectrometry, the protein bands of interest were excised, subjected to digestion with trypsin or chymotrypsin, and analyzed by electrospray ionization tandem mass spectrometry (MS/MS).

Online supplemental material

Fig. S1 shows optimization of the sortase-mediated reactions to label CTA1 in the context of the holotoxin. Fig. S2 shows mass spectrometry data on the identity of the CTx–DTA conjugate. Table S1 shows the DNA sequences flanking each of the retroviral insertion sites. Table S2 shows the data analysis for the results obtained in the genetic screen. Online supplemental material is available at http://www.jcb.org/cgi/content/full/jcb.201108103/DC1.

We thank T. DiCesare for graphics support, and C. Araneo and E. Guillen for help with FACS sorting and FACS analysis.

C.P. Guimaraes was supported by a fellowship from Fundacao Ciencia Tecnologia, Portugal.

Submitted: 16 August 2011
Accepted: 28 October 2011

References

Allured, V.S., R.J. Collier, S.F. Carroll, and D.B. McKay. 1986. Structure of exotoxin A of *Pseudomonas aeruginosa* at 3.0-Angstrom resolution. *Proc. Natl. Acad. Sci. USA*. 83:1320–1324. http://dx.doi.org/10.1073/pnas.83.5.1320

Antos, J.M., G.M. Miller, G.M. Grotenbreg, and H.L. Ploegh. 2008. Lipid modification of proteins through sortase-catalyzed transpeptidation. *J. Am. Chem. Soc.* 130:16338–16343. http://dx.doi.org/10.1021/ja806779e

Antos, J.M., M.W. Popp, R. Ernst, G.L. Chew, E. Spooner, and H.L. Ploegh. 2009. A straight path to circular proteins. *J. Biol. Chem.* 284:16028–16036. http://dx.doi.org/10.1074/jbc.M901752200

Arunachalam, B., U.T. Phan, H.J. Geuze, and P. Cresswell. 2000. Enzymatic reduction of disulfide bonds in lysosomes: characterization of a gamma-interferon-inducible lysosomal thiol reductase (GILT). *Proc. Natl. Acad. Sci. USA*. 97:745–750. http://dx.doi.org/10.1073/pnas.97.2.745

Bacia, K., I.V. Majoul, and P. Schwille. 2002. Probing the endocytic pathway in live cells using dual-color fluorescence cross-correlation analysis. *Biophys. J.* 83:1184–1193. http://dx.doi.org/10.1016/S0006-3495(02)75242-9

Bastiaens, P.I., I.V. Majoul, P.J. Verveer, H.D. Söling, and T.M. Jovin. 1996. Imaging the intracellular trafficking and state of the AB5 quaternary structure of cholera toxin. *EMBO J.* 15:4246–4253.

Bernardi, K.M., M.L. Forster, W.I. Lencer, and B. Tsai. 2008. Derlin-1 facilitates the retro-translocation of cholera toxin. *Mol. Biol. Cell*. 19:877–884. http://dx.doi.org/10.1091/mbc.E07-08-0755

Bernardi, K.M., J.M. Williams, M. Kikkert, S. van Voorden, E.J. Wiertz, Y. Ye, and B. Tsai. 2010. The E3 ubiquitin ligases Hrd1 and gp78 bind to and promote cholera toxin retro-translocation. *Mol. Biol. Cell*. 21:140–151. http://dx.doi.org/10.1091/mbc.E09-07-0586

Carette, J.E., C.P. Guimaraes, M. Varadarajan, A.S. Park, I. Wuethrich, A. Godarova, M. Kotecki, B.H. Cochran, E. Spooner, H.L. Ploegh, and T.R. Brummelkamp. 2009. Haploid genetic screens in human cells identify host factors used by pathogens. *Science*. 326:1231–1235. http://dx.doi.org/10.1126/science.1178955

Carette, J.E., C.P. Guimaraes, I. Wuethrich, V.A. Blomen, M. Varadarajan, C. Sun, G. Bell, B. Yuan, M.K. Muellner, S.M. Nijman, et al. 2011. Global gene disruption in human cells to assign genes to phenotypes by deep sequencing. *Nat. Biotechnol.* 29:542–546. http://dx.doi.org/10.1038/nbt.1857

Chaudhary, V.K., Y. Jinno, D. FitzGerald, and I. Pastan. 1990. *Pseudomonas* exotoxin contains a specific sequence at the carboxyl terminus that is required for cytotoxicity. *Proc. Natl. Acad. Sci. USA*. 87:308–312. http://dx.doi.org/10.1073/pnas.87.1.308

Chen, I., M. Howarth, W. Lin, and A.Y. Ting. 2005. Site-specific labeling of cell surface proteins with biophysical probes using biotin ligase. *Nat. Methods*. 2:99–104. http://dx.doi.org/10.1038/nmeth735

Collier, R.J. 2001. Understanding the mode of action of diphtheria toxin: a perspective on progress during the 20th century. *Toxicon*. 39:1793–1803. http://dx.doi.org/10.1016/S0041-0101(01)00165-9

Dertzbaugh, M.T., and L.M. Cox. 1998. The affinity of cholera toxin for Ni2+ ion. *Protein Eng.* 11:577–581. http://dx.doi.org/10.1093/protein/11.7.577

Dixit, G., C. Mikoryak, T. Hayslett, A. Bhat, and R.K. Draper. 2008. Cholera toxin up-regulates endoplasmic reticulum proteins that correlate with sensitivity to the toxin. *Exp. Biol. Med. (Maywood)*. 233:163–175. http://dx.doi.org/10.3181/0705-RM-132

Doms, R.W., G. Russ, and J.W. Yewdell. 1989. Brefeldin A redistributes resident and itinerant Golgi proteins to the endoplasmic reticulum. *J. Cell Biol.* 109:61–72. http://dx.doi.org/10.1083/jcb.109.1.61

Donta, S.T., S.R. Kreiter, and G. Wendelschafer-Crabb. 1976. Morphological and steroidogenic changes in cultured adrenal tumor cells induced by a subunit of cholera enterotoxin. *Infect. Immun.* 13:1479–1482.

Dougan, S.K., C.C. Hu, M.E. Paquet, M.B. Greenblatt, J. Kim, B.N. Lilley, N. Watson, and H.L. Ploegh. 2011. Derlin-2-deficient mice reveal an essential role for protein dislocation in chondrocytes. *Mol. Cell. Biol.* 31:1145–1159. http://dx.doi.org/10.1128/MCB.00967-10

Fraser, M.E., M.M. Chernaia, Y.V. Kozlov, and M.N. James. 1994. Crystal structure of the holotoxin from *Shigella dysenteriae* at 2.5 A resolution. *Nat. Struct. Biol.* 1:59–64. http://dx.doi.org/10.1038/nsb0194-59

Fujinaga, Y., A.A. Wolf, C. Rodighiero, H. Wheeler, B. Tsai, L. Allen, M.G. Jobling, T. Rapoport, R.K. Holmes, and W.I. Lencer. 2003. Gangliosides that associate with lipid rafts mediate transport of cholera and related toxins from the plasma membrane to endoplasmic reticulm. *Mol. Biol. Cell*. 14:4783–4793. http://dx.doi.org/10.1091/mbc.E03-06-0354

Guerrant, R.L., L.L. Brunton, T.C. Schnaitman, L.I. Rebhun, and A.G. Gilman. 1974. Cyclic adenosine monophosphate and alteration of Chinese hamster ovary cell morphology: a rapid, sensitive in vitro assay for the enterotoxins of *Vibrio cholerae* and *Escherichia coli*. *Infect. Immun.* 10:320–327.

Hazes, B., and R.J. Read. 1997. Accumulating evidence suggests that several AB-toxins subvert the endoplasmic reticulum-associated protein degradation pathway to enter target cells. *Biochemistry*. 36:11051–11054. http://dx.doi.org/10.1021/bi971383p

Heyningen, S.V. 1974. Cholera toxin: interaction of subunits with ganglioside GM1. *Science*. 183:656–657. http://dx.doi.org/10.1126/science.183.4125.656

Jobling, M.G., and R.K. Holmes. 2000. Identification of motifs in cholera toxin A1 polypeptide that are required for its interaction with human ADP-ribosylation factor 6 in a bacterial two-hybrid system. *Proc. Natl. Acad. Sci. USA*. 97:14662–14667. http://dx.doi.org/10.1073/pnas.011442598

Jobling, M.G., and R.K. Holmes. 2001. Biological and biochemical characterization of variant A subunits of cholera toxin constructed by site-directed mutagenesis. *J. Bacteriol.* 183:4024–4032. http://dx.doi.org/10.1128/JB.183.13.4024-4032.2001

Jobling, M.G., L.M. Palmer, J.L. Erbe, and R.K. Holmes. 1997. Construction and characterization of versatile cloning vectors for efficient delivery of native foreign proteins to the periplasm of *Escherichia coli*. *Plasmid*. 38:158–173. http://dx.doi.org/10.1006/plas.1997.1309

Kahn, R.A., and A.G. Gilman. 1984. ADP-ribosylation of Gs promotes the dissociation of its alpha and beta subunits. *J. Biol. Chem.* 259:6235–6240.

Kassis, S., J. Hagmann, P.H. Fishman, P.P. Chang, and J. Moss. 1982. Mechanism of action of cholera toxin on intact cells. Generation of A1 peptide and activation of adenylate cyclase. *J. Biol. Chem.* 257:12148–12152.

Keppler, A., S. Gendreizig, T. Gronemeyer, H. Pick, H. Vogel, and K. Johnsson. 2003. A general method for the covalent labeling of fusion proteins with small molecules in vivo. *Nat. Biotechnol.* 21:86–89. http://dx.doi.org/10.1038/nbt765

Lencer, W.I., and B. Tsai. 2003. The intracellular voyage of cholera toxin: going retro. *Trends Biochem. Sci.* 28:639–645. http://dx.doi.org/10.1016/j.tibs.2003.10.002

Lencer, W.I., C. Delp, M.R. Neutra, and J.L. Madara. 1992. Mechanism of cholera toxin action on a polarized human intestinal epithelial cell line: role of

vesicular traffic. *J. Cell Biol.* 117:1197–1209. http://dx.doi.org/10.1083/jcb.117.6.1197

Lencer, W.I., J.B. de Almeida, S. Moe, J.L. Stow, D.A. Ausiello, and J.L. Madara. 1993. Entry of cholera toxin into polarized human intestinal epithelial cells. Identification of an early brefeldin A sensitive event required for A1-peptide generation. *J. Clin. Invest.* 92:2941–2951. http://dx.doi.org/10.1172/JCI116917

Lencer, W.I., C. Constable, S. Moe, M.G. Jobling, H.M. Webb, S. Ruston, J.L. Madara, T.R. Hirst, and R.K. Holmes. 1995. Targeting of cholera toxin and *Escherichia coli* heat labile toxin in polarized epithelia: role of COOH-terminal KDEL. *J. Cell Biol.* 131:951–962. http://dx.doi.org/10.1083/jcb.131.4.951

Lippincott-Schwartz, J., L.C. Yuan, J.S. Bonifacino, and R.D. Klausner. 1989. Rapid redistribution of Golgi proteins into the ER in cells treated with brefeldin A: evidence for membrane cycling from Golgi to ER. *Cell*. 56:801–813. http://dx.doi.org/10.1016/0092-8674(89)90685-5

Liu, S., G.T. Milne, J.G. Kuremsky, G.R. Fink, and S.H. Leppla. 2004. Identification of the proteins required for biosynthesis of diphthamide, the target of bacterial ADP-ribosylating toxins on translation elongation factor 2. *Mol. Cell. Biol.* 24:9487–9497. http://dx.doi.org/10.1128/MCB.24.21.9487-9497.2004

Liu, Y., Y. Su, M. Wiznitzer, O. Epifano, and S. Ladisch. 2008. Ganglioside depletion and EGF responses of human GM3 synthase-deficient fibroblasts. *Glycobiology*. 18:593–601. http://dx.doi.org/10.1093/glycob/cwn039

Maccioni, H.J., R. Quiroga, and M.L. Ferrari. 2011. Cellular and molecular biology of glycosphingolipid glycosylation. *J. Neurochem.* 117:589–602.

Maglione, V., P. Marchi, A. Di Pardo, S. Lingrell, M. Horkey, E. Tidmarsh, and S. Sipione. 2010. Impaired ganglioside metabolism in Huntington's disease and neuroprotective role of GM1. *J. Neurosci.* 30:4072–4080. http://dx.doi.org/10.1523/JNEUROSCI.6348-09.2010

Majoul, I., D. Ferrari, and H.D. Söling. 1997. Reduction of protein disulfide bonds in an oxidizing environment. The disulfide bridge of cholera toxin A-subunit is reduced in the endoplasmic reticulum. *FEBS Lett.* 401:104–108. http://dx.doi.org/10.1016/S0014-5793(96)01447-0

Majoul, I., T. Schmidt, M. Pomasanova, E. Boutkevich, Y. Kozlov, and H.D. Söling. 2002. Differential expression of receptors for Shiga and Cholera toxin is regulated by the cell cycle. *J. Cell Sci.* 115:817–826.

Mekalanos, J.J., R.J. Collier, and W.R. Romig. 1979. Enzymic activity of cholera toxin. II. Relationships to proteolytic processing, disulfide bond reduction, and subunit composition. *J. Biol. Chem.* 254:5855–5861.

Milne, J.C., S.R. Blanke, P.C. Hanna, and R.J. Collier. 1995. Protective antigen-binding domain of anthrax lethal factor mediates translocation of a heterologous protein fused to its amino- or carboxy-terminus. *Mol. Microbiol.* 15:661–666. http://dx.doi.org/10.1111/j.1365-2958.1995.tb02375.x

Miyazaki, Y., X. Sun, H. Uchida, J. Zhang, and S. Nimer. 1996. MEF, a novel transcription factor with an Elf-1 like DNA binding domain but distinct transcriptional activating properties. *Oncogene*. 13:1721–1729.

Naglich, J.G., J.E. Metherall, D.W. Russell, and L. Eidels. 1992. Expression cloning of a diphtheria toxin receptor: identity with a heparin-binding EGF-like growth factor precursor. *Cell*. 69:1051–1061. http://dx.doi.org/10.1016/0092-8674(92)90623-K

Nambiar, M.P., T. Oda, C. Chen, Y. Kuwazuru, and H.C. Wu. 1993. Involvement of the Golgi region in the intracellular trafficking of cholera toxin. *J. Cell. Physiol.* 154:222–228. http://dx.doi.org/10.1002/jcp.1041540203

Navarre, W.W., and O. Schneewind. 1994. Proteolytic cleavage and cell wall anchoring at the LPXTG motif of surface proteins in gram-positive bacteria. *Mol. Microbiol.* 14:115–121. http://dx.doi.org/10.1111/j.1365-2958.1994.tb01271.x

Nery, F.C., I.A. Armata, J.E. Farley, J.A. Cho, U. Yaqub, P. Chen, C.C. da Hora, Q. Wang, M. Tagaya, C. Klein, et al. 2011. TorsinA participates in endoplasmic reticulum-associated degradation. *Nat Commun*. 2:393. http://dx.doi.org/10.1038/ncomms1383

Nesić, D., Y. Hsu, and C.E. Stebbins. 2004. Assembly and function of a bacterial genotoxin. *Nature*. 429:429–433. http://dx.doi.org/10.1038/nature02532

Orlandi, P.A. 1997. Protein-disulfide isomerase-mediated reduction of the A subunit of cholera toxin in a human intestinal cell line. *J. Biol. Chem.* 272:4591–4599.

Orlandi, P.A., P.K. Curran, and P.H. Fishman. 1993. Brefeldin A blocks the response of cultured cells to cholera toxin. Implications for intracellular trafficking in toxin action. *J. Biol. Chem.* 268:12010–12016.

Pande, A.H., P. Scaglione, M. Taylor, K.N. Nemec, S. Tuthill, D. Moe, R.K. Holmes, S.A. Tatulian, and K. Teter. 2007. Conformational instability of the cholera toxin A1 polypeptide. *J. Mol. Biol.* 374:1114–1128. http://dx.doi.org/10.1016/j.jmb.2007.10.025

Popp, M.W., and H.L. Ploegh. 2011. Making and breaking peptide bonds: protein engineering using sortase. *Angew. Chem. Int. Ed. Engl.* 50:5024–5032. http://dx.doi.org/10.1002/anie.201008267

Popp, M.W., J.M. Antos, G.M. Grotenbreg, E. Spooner, and H.L. Ploegh. 2007. Sortagging: a versatile method for protein labeling. *Nat. Chem. Biol.* 3:707–708. http://dx.doi.org/10.1038/nchembio.2007.31

Rapak, A., P.O. Falnes, and S. Olsnes. 1997. Retrograde transport of mutant ricin to the endoplasmic reticulum with subsequent translocation to cytosol. *Proc. Natl. Acad. Sci. USA*. 94:3783–3788. http://dx.doi.org/10.1073/pnas.94.8.3783

Saslowsky, D.E., J.A. Cho, H. Chinnapen, R.H. Massol, D.J. Chinnapen, J.S. Wagner, H.E. De Luca, W. Kam, B.H. Paw, and W.I. Lencer. 2010. Intoxication of zebrafish and mammalian cells by cholera toxin depends on the flotillin/reggie proteins but not Derlin-1 or -2. *J. Clin. Invest.* 120:4399–4409. http://dx.doi.org/10.1172/JCI42958

Schafer, D.E., W.D. Lust, B. Sircar, and N.D. Goldberg. 1970. Elevated concentration of adenosine 3′:5′-cyclic monophosphate in intestinal mucosa after treatment with cholera toxin. *Proc. Natl. Acad. Sci. USA*. 67:851–856. http://dx.doi.org/10.1073/pnas.67.2.851

Schmitz, A., H. Herrgen, A. Winkeler, and V. Herzog. 2000. Cholera toxin is exported from microsomes by the Sec61p complex. *J. Cell Biol.* 148:1203–1212. http://dx.doi.org/10.1083/jcb.148.6.1203

Shevchuk, N.A., Y. Hathout, O. Epifano, Y. Su, Y. Liu, M. Sutherland, and S. Ladisch. 2007. Alteration of ganglioside synthesis by GM3 synthase knockout in murine embryonic fibroblasts. *Biochim. Biophys. Acta*. 1771:1226–1234.

Simpson, M.A., H. Cross, C. Proukakis, D.A. Priestman, D.C. Neville, G. Reinkensmeier, H. Wang, M. Wiznitzer, K. Gurtz, A. Verganelaki, et al. 2004. Infantile-onset symptomatic epilepsy syndrome caused by a homozygous loss-of-function mutation of GM3 synthase. *Nat. Genet.* 36:1225–1229. http://dx.doi.org/10.1038/ng1460

Sixma, T.K., S.E. Pronk, K.H. Kalk, E.S. Wartna, B.A. van Zanten, B. Witholt, and W.G. Hol. 1991. Crystal structure of a cholera toxin-related heat-labile enterotoxin from *E. coli. Nature*. 351:371–377. http://dx.doi.org/10.1038/351371a0

Taylor, M., T. Banerjee, S. Ray, S.A. Tatulian, and K. Teter. 2011. Protein-disulfide isomerase displaces the cholera toxin A1 subunit from the holotoxin without unfolding the A1 subunit. *J. Biol. Chem.* 286:22090–22100. http://dx.doi.org/10.1074/jbc.M111.237966

Teter, K., and R.K. Holmes. 2002. Inhibition of endoplasmic reticulum-associated degradation in CHO cells resistant to cholera toxin, *Pseudomonas aeruginosa* exotoxin A, and ricin. *Infect. Immun.* 70:6172–6179. http://dx.doi.org/10.1128/IAI.70.11.6172-6179.2002

Teter, K., R.L. Allyn, M.G. Jobling, and R.K. Holmes. 2002. Transfer of the cholera toxin A1 polypeptide from the endoplasmic reticulum to the cytosol is a rapid process facilitated by the endoplasmic reticulum-associated degradation pathway. *Infect. Immun.* 70:6166–6171. http://dx.doi.org/10.1128/IAI.70.11.6166-6171.2002

Ton-That, H., G. Liu, S.K. Mazmanian, K.F. Faull, and O. Schneewind. 1999. Purification and characterization of sortase, the transpeptidase that cleaves surface proteins of *Staphylococcus aureus* at the LPXTG motif. *Proc. Natl. Acad. Sci. USA*. 96:12424–12429. http://dx.doi.org/10.1073/pnas.96.22.12424

Tsai, B., C. Rodighiero, W.I. Lencer, and T.A. Rapoport. 2001. Protein disulfide isomerase acts as a redox-dependent chaperone to unfold cholera toxin. *Cell*. 104:937–948. http://dx.doi.org/10.1016/S0092-8674(01)00289-6

Tsukiji, S., and T. Nagamune. 2009. Sortase-mediated ligation: a gift from Gram-positive bacteria to protein engineering. *ChemBioChem*. 10:787–798. http://dx.doi.org/10.1002/cbic.200800724

Wernick, N.L., H. De Luca, W.R. Kam, and W.I. Lencer. 2010a. N-terminal extension of the cholera toxin A1-chain causes rapid degradation after retrotranslocation from endoplasmic reticulum to cytosol. *J. Biol. Chem.* 285:6145–6152. http://dx.doi.org/10.1074/jbc.M109.062067

Wernick, N.L.B., D.-F. Chinnapen, J.A. Cho, and W.I. Lencer. 2010b. Cholera toxin: an intracellular journey into the cytosol by way of the endoplasmic reticulum. *Toxins*. 2:310–325. http://dx.doi.org/10.3390/toxins2030310

Winkeler, A., D. Gödderz, V. Herzog, and A. Schmitz. 2003. BiP-dependent export of cholera toxin from endoplasmic reticulum-derived microsomes. *FEBS Lett.* 554:439–442. http://dx.doi.org/10.1016/S0014-5793(03)01217-1

Yamashita, T., A. Hashiramoto, M. Haluzik, H. Mizukami, S. Beck, A. Norton, M. Kono, S. Tsuji, J.L. Daniotti, N. Werth, et al. 2003. Enhanced insulin sensitivity in mice lacking ganglioside GM3. *Proc. Natl. Acad. Sci. USA*. 100:3445–3449. http://dx.doi.org/10.1073/pnas.0635898100

Yoshida, T., C.C. Chen, M.S. Zhang, and H.C. Wu. 1991. Disruption of the Golgi apparatus by brefeldin A inhibits the cytotoxicity of ricin, modeccin, and *Pseudomonas* toxin. *Exp. Cell Res.* 192:389–395. http://dx.doi.org/10.1016/0014-4827(91)90056-Z

Zhang, R.G., D.L. Scott, M.L. Westbrook, S. Nance, B.D. Spangler, G.G. Shipley, and E.M. Westbrook. 1995. The three-dimensional crystal structure of cholera toxin. *J. Mol. Biol.* 251:563–573. http://dx.doi.org/10.1006/jmbi.1995.0456